PROCEEDINGS OF SPIE

SPIEDigitalLibrary.org/conference-proceedings-of-spie

Temporal dynamics of frequency-tunable graphene-based plasmonic grating structures for ultra-broadband terahertz communication

Jornet, Josep Miquel, Thawdar, Ngwe, Woo, Ethan, Andrello, Michael

Josep Miquel Jornet, Ngwe Thawdar, Ethan Woo, Michael A. Andrello III, "Temporal dynamics of frequency-tunable graphene-based plasmonic grating structures for ultra-broadband terahertz communication," Proc. SPIE 10206, Disruptive Technologies in Sensors and Sensor Systems, 1020608 (2 May 2017); doi: 10.1117/12.2262885

SPIE.

Event: SPIE Defense + Security, 2017, Anaheim, California, United States

Temporal Dynamics of Frequency-tunable Graphene-based Plasmonic Grating Structures for Ultra-broadband Terahertz Communication

Josep Miquel Jornet[a], Ngwe Thawdar[b], Ethan Woo[c], and Michael A. Andrello III[d]

[a]Department of Electrical Engineering, University at Buffalo (SUNY), Buffalo, NY, USA
[b]Air Force Research Laboratory/RI, Rome, NY, USA
[c]SUNY Polytechnic College of Nanoscale Science and Engineering (CNSE), Albany, NY, USA
[d]Department of Materials Science and Engineering, Virginia Tech, Blacksburg, VA, USA

ABSTRACT

Terahertz (THz) communication is envisioned as a key wireless technology to satisfy the need for 1000x faster wireless data rates. To date, major progress on both electronic and photonic technologies are finally closing the so-called THz gap. Among others, graphene-based plasmonic nano-devices have been proposed as a way to enable ultra-broadband communications above 1 THz. The unique dynamic complex conductivity of graphene enables the propagation of Surface Plasmon Polariton (SPP) waves at THz frequencies. In addition, the conductivity of graphene and, thus, the SPP propagation properties, can be dynamically tuned by means of electrostatic biasing or material doping. This result opens the door to frequency-tunable devices for THz communications. In this paper, the temporal dynamics of graphene-enhanced metallic grating structures used for excitation and detection of SPP waves at THz frequencies are analytically and numerically modeled. More specifically, the response of a metallic grating structure built on top of a graphene-based heterostructure is analyzed by taking into account the grating period and duty cycle and the Fermi energy of the graphene layer. Then, the interfacial charge transfer between a metallic back-gate and the graphene layer in a metal/dielectric/graphene stack is analytically modeled, and the range of achievable Fermi energies is determined. Finally, the rate at which the Fermi energy in graphene can be tuned is estimated starting from the transmission line model of graphene. Extensive numerical and simulation results with COMSOL Multi-physics are provided. The results show that the proposed structure enables dynamic frequency systems with THz bandwidths, thus, enabling resilient communication techniques such as time-hopping THz modulations.

Keywords: Terahertz Communications, Graphene Plasmonics, Grating Structures

1. INTRODUCTION

Wireless data rates have doubled every 18 months for the last three decades.[1] Following this trend, Terabit-per-second (Tbps) links will become a reality within the next five years. Several alternatives are being considered to meet this demand. At frequencies below 5 GHz, advanced digital modulations and sophisticated physical layer schemes are being used to achieve a very high spectral efficiency. However, the very small bandwidth available in the overcrowded electromagnetic (EM) spectrum limits the achievable data rates. Millimeter-wave (mm-wave) communication systems (30 to 300 GHz) have gained a lot of attention in the last few years due to their ability to support much higher rates than communication systems below 5 GHz.[2] While on the right track, the total consecutive available bandwidth for mm-wave communication systems is still less than 10 GHz and, thus, would require physical layer efficiency of almost 100 bit/s/Hz, which is several times higher than the state of the art for existing systems. This result motivates further research and the exploration of even higher frequency bands. Optical wireless communication (OWC) systems are similarly being explored as a way to improve the achievable data rates.[3] However, several aspects limit OWC systems, including the size and limited portability of infrared systems or the impact of ambient noise in visible communication.

Further author information: (Send correspondence to J. M. J.)
J.M.J.: E-mail: jmjornet@buffalo.edu

Disruptive Technologies in Sensors and Sensor Systems, edited by Russell D. Hall, Misty Blowers, Jonathan Williams,
Proc. of SPIE Vol. 10206, 1020608 · © 2017 SPIE · CCC code: 0277-786X/17/$18 · doi: 10.1117/12.2262885

In this context, Terahertz-band (0.1 to 10 THz) communication has been envisioned as a key wireless technology to satisfy the need for much higher wireless data rates.[4–7] The THz band supports huge transmission bandwidths, which range from almost 10 THz for distances below one meter, to multiple transmission windows, each tens to hundreds of GHz wide, for distances on the order of a few tens of meters. Nevertheless, this very large bandwidth comes at the cost of a very high propagation loss, mainly affected by the absorption from water vapor molecules.[8] For many decades, the lack of compact high-power signal sources and high-sensitivity detectors able to work at room temperature has hampered the use of the THz band for any application beyond sensing. However, many recent technological advancements are finally closing the so-called THz gap.

In an electronic approach, III–V semiconductor technologies, such as indium phosphide heterojunction bipolar transistor technology, have demonstrated record performance in terms of output power, noise figure, and power-added efficiency at sub-THz frequencies, and are quickly approaching the 1 THz mark.[9–11] These systems commonly rely on frequency-multiplying chains to up-convert a multi-GHz local oscillator to THz frequencies. Power loss due to the generation of non-desired harmonics and limited gain of these devices when approaching true THz frequencies hamper the energy efficiency and limit the feasibility of this technology for higher frequencies. In an optics approach or optoelectronic approach, quantum cascade lasers (QCLs) are clear potential candidates for high-power THz-band signal generation.[12–14] These lasers can yield THz emission across a broad spectrum, offering output in the range of tens of milliwatts at cryogenic temperatures. However, they suffer from poor performance at room temperature, which limits their application in practical scenarios.

A promising approach to realizing THz communications is to leverage the properties of plasmonic materials. For example, THz-frequency plasmons can be generated in the channel of a high-electron-mobility transistor (HEMT) by means of electrical or optical pumping.[15–17] These plasmons are sustainable at cryogenic temperatures, but quickly decay at room temperature due to phonon-induced overdamping. Moreover, efficiently radiating these plasma excitations directly from the HEMT has proven difficult, but there is room for improvement. In this direction, the use of plasmonic nanomaterials such as graphene has been proposed. Graphene is a two-dimensional carbon material that has excellent electrical conductivity, making it very well suited for propagating extremely-high-frequency electrical signals.[18–20] Moreover, graphene supports the propagation of THz surface plasmon polariton (SPP) waves. This is a very unique property, as SPP waves only propagate in conventional plasmonic materials in the infra-red and above. In addition, the SPP wave propagation properties can be dynamically tuned by changing the graphene conductivity, which leads to reconfigurable devices.[21]

There are different mechanisms to excite SPP waves on graphene. In Reference,[22] we proposed a novel hybrid graphene/ semiconductor HEMT structure which can electrically excite SPP on graphene. The working principle of the proposed device relies on the Dyakonov-Shur instability[15,23] to excite a plasma wave in the HEMT channel, which then is utilized to launch a SPP wave on the graphene layer. In this design, the tunability of the graphene layer Fermi energy is leveraged to maximize the coupling between the plasma wave and the SPP wave. Another mechanism to excite SPP waves on graphene relies on the use of grating gated structures. For example, illuminating a grating-gated structure with a QCL would result in a SPP wave that propagates well beyond the gated cavity.[24,25] The grating structure performs two critical functions. First, it provides effective coupling between the THz EM wave and the plasma excitations in graphene by eliminating the momentum mismatch between the THz photon and the graphene plasmon. Second, the grating gate allows controlled changes of the electron density in the graphene by varying the gate voltage applied between the gate and the graphene channel.

Besides the THz signal source and detector, a key element to enable practical THz communication systems is the modulator. As mentioned before, a key advantage of the THz band is its very large usable bandwidth, ranging from hundreds of GHz and up to a few THz. To benefit from such bandwidth, signal modulating devices with equally large modulation bandwidths are needed. The use of graphene to develop THz wave modulators has been proposed.[26–28] In these designs, the fundamental idea is to modulate the amplitude or phase of a propagating THz signal by dynamically tuning the conductivity of graphene. In a grating gated structure, such property can be exploited in two ways. On the one hand, by changing the Fermi energy, the plasmonic structure can be tuned in or out of resonance, thus, enabling amplitude modulation. On the other hand, the frequency of the THz SPP Wave on graphene can be dynamically changed, enabling massive frequency division multiplexing systems at THz frequencies. In any case, the speed at which the Fermi energy can be changed determines the modulation bandwidth, which remains unclear.

In this paper, we analytically and numerically investigate the temporal dynamics of graphene-enhanced metallic grating structures used for excitation and detection of SPP waves at THz frequencies. More specifically, the response of a metallic grating structure built on top of a graphene-based heterostructure is analyzed by taking into account the grating period and duty cycle and the Fermi energy of the graphene layer (Section 2). Extensive simulations with COMSOL Multi-physics are provided to validate the theoretical models. Second, the interfacial charge transfer between a metallic back-gate and the graphene layer in a metal/dielectric/graphene stack is analytically modeled, and the range of achievable Fermi energies is determined. In addition, the rate at which the Fermi energy in graphene can be tuned is estimated starting from the transmission line model of graphene (Section 3). The results show that the proposed structure enables dynamic frequency systems with THz bandwidths, thus, enabling resilient communication techniques such as time-hopping THz modulations.

2. GRATING-GATED GRAPHENE-BASED HETEROSTRUCTURES

In this section, we analytically model the generation of SPP waves in grating-gated graphene-based structures and provide extensive numerical simulations to analyze the impact of different grating parameters on frequency and coupling efficiency.

2.1 Theoretical Modeling

A conceptual illustration of the grating-gated graphene-based heterostructures under analysis is shown in Figure 1. In this design, the graphene layer rests on top of a dielectric (silicon dioxide, SiO_2) and PMMA separates the graphene layer from a gold grating structure. In our analysis, we consider a surface conductivity model for infinitely large graphene sheets obtained using the Kubo formalism.[29,30] This is given by

$$\sigma^g = \sigma^g_{\text{intra}} + \sigma^g_{\text{inter}}, \tag{1}$$

$$\sigma^g_{\text{intra}} = i\frac{2e^2}{\pi\hbar^2}\frac{k_B T}{\omega + i\tau_g^{-1}} \ln\left(2\cosh\left(\frac{E_F}{2k_B T}\right)\right), \tag{2}$$

$$\sigma^g_{\text{inter}} = \frac{e^2}{4\hbar}\left(H\left(\frac{\omega}{2}\right) + \mathrm{i}\frac{4\omega}{\pi}\int_0^\infty \frac{G(\epsilon) - G(\omega/2)}{\omega^2 - 4\epsilon^2}\, d\epsilon\right), \tag{3}$$

and

$$G(a) = \frac{\sinh(\hbar a/k_B T)}{\cosh(E_F/k_B T) + \cosh(\hbar a/k_B T)}, \tag{4}$$

where $\omega = 2\pi f$, $\hbar = h/2\pi$ is the reduced Planck's constant, e is the electron charge, k_B is the Boltzmann constant, T is temperature, E_F refers to the Fermi energy of the graphene sheet, and τ_g is the relaxation time of electrons in graphene, which depends on the electron mobility μ_g. E_F can be easily modified by means of electrostatic bias through the grating gated structure and, thus, enabling the modulation of the structure response.

The SPP wave properties, including resonant frequency and amplitude, are determined by the SPP wavevector k_{spp}, which can be then obtained by solving the dispersion equation in this structure. Analytical closed-form expressions for these two parameters exist only for simplified grating gated geometries.[31,32] In this paper, we will instead investigate the impact of the grating geometry and the Fermi energy of the graphene layer on the SPP wave properties by means of full-wave simulations.

2.2 Full-wave Analysis

We utilize COMSOL Multi-physics[33] to simulate the grating-gated graphene-based plasmonic heterostructure show in Figure 1. Graphene is modeled as a transition boundary condition with complex dynamic conductivity given by (1), where $\tau_g = 0.5\,\text{ps}$ and tunable Fermi energy between $E_F = 0.1$ to $1\,\text{eV}$ at $T = 300\,\text{K}$. These values are based on analysis of Raman spectra obtained from CVD-grown graphene. The graphene layer rests on top of a several-micrometer-thick SiO_2 dielectric ($\varepsilon_r = 2.2$). A $45\,\text{nm}$-thick PMMA layer ($\varepsilon_r = 3.2$) separates the

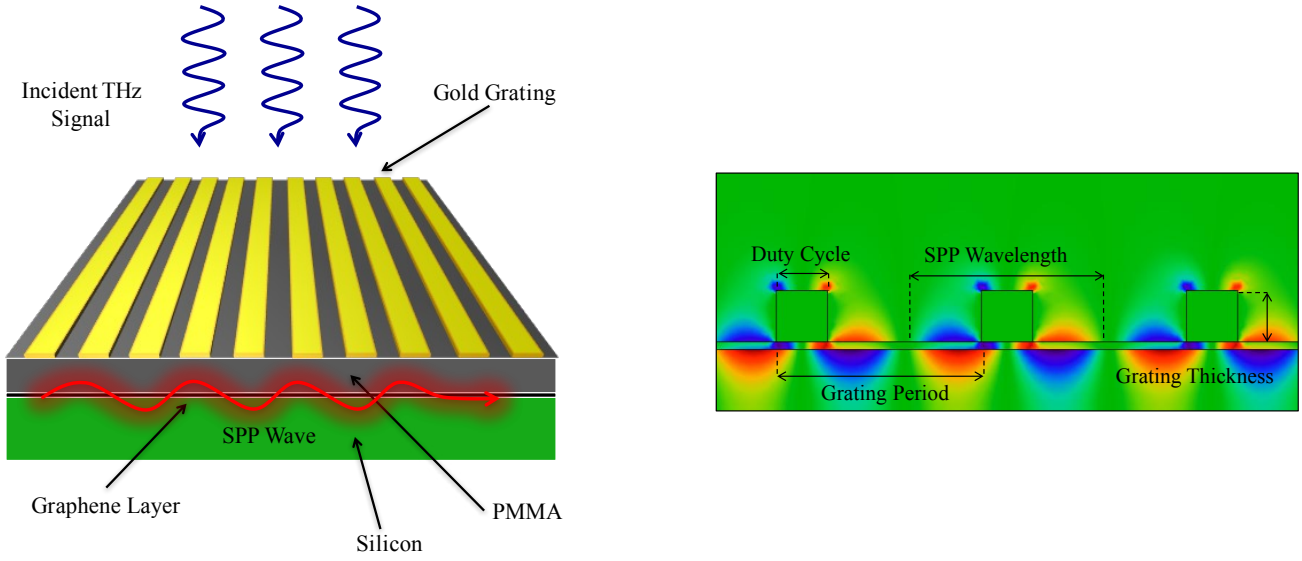

(a) (b)

Figure 1: a) Conceptual illustration of a grating-gated graphene-based plasmonic heterostructure. b) Geometry and relevant dimensions.

graphene layer from the gold grating. The conductivity of gold is modeled with the well-established Drude model and the values in Reference 34. A perfectly matched layer and a scattering boundary condition are utilized to minimize the impact of simulating a finite space. The antenna is meshed with a resolution of $\lambda_{spp}/5$, where λ_{spp} refers to the plasmonic wavelength.

First, we investigate the impact of the grating period on the SPP wave resonance frequency. For this study, we consider a 300 nm-thick grating, with a 200 nm duty cycle, a 45 nm-thick PMMA layer, and a Fermi energy of 0.2 eV. The range of the grating period was from 300 to 1600 nm. In Figure 2, we illustrate the incident (first order) resonant frequency and the resulting SPP wavelength, amplitude and confinement factor (k_{spp}/k, where k is the incident wavevector) as functions on the grating period. For a fixed Fermi energy, the grating period determines the incident resonant frequency, which decreases with the grating period. The SPP wavelength at the resonant frequency increases with the grating period. This is a result of having a less confined SPP wave, which also has a lower amplitude. These results are consistent with the existing related literature.[24,25,32]

Second, we investigate the impact of the Fermi energy of the graphene layer on the device performance. The Fermi energy can be controlled by utilizing the grating structure as a top gate. In this study, the grating period length is fixed at 1600 nm with a duty cycle of 200 nm and a thickness of 300 nm on top of a 45 nm-thick PMMA layer above the graphene layer. The Fermi energy ranges from 0.01 to 0.2 eV. In this scenario, for a fixed geometrical structure of the device, we can electronically tune the incident frequency at which the resonance occurs. In particular, the incident resonant frequency increases with the Fermi energy. In accordance with our previous studies,[35] an increase in the Fermi energy leads to a lower SPP confinement factor and this turns into a higher SPP amplitude. This is opposed to the results in Figure 2, in which a decrease in the confinement factor leads to a weaker SPP wave. This result can be understood as follows. The grating period is controlling the coupling between the free-space photon and the graphene plasmon, whereas the Fermi energy is controlling the ease with which such SPP wave propagates. Theoretically, at E_F =0 eV, the confinement factor tends to infinity with an amplitude that tends to zero (but in any case, the conductivity model does not hold in such case).

As part of our analysis, we are also interested to know the propagation length or the amplitude decay of the SPP wave, in the case of having the grating gate only on a portion of the graphene-based heterostructure. This will be the case, for example, in which a QCL is utilized to excite a SPP wave, but then that SPP wave propagates further from the source to a plasmonic modulator[28] or plasmonic antenna.[35] In this study, we simulate a device with the exact same grating configuration as in the previous case (period of 1600 nm, duty cycle of 200 nm,

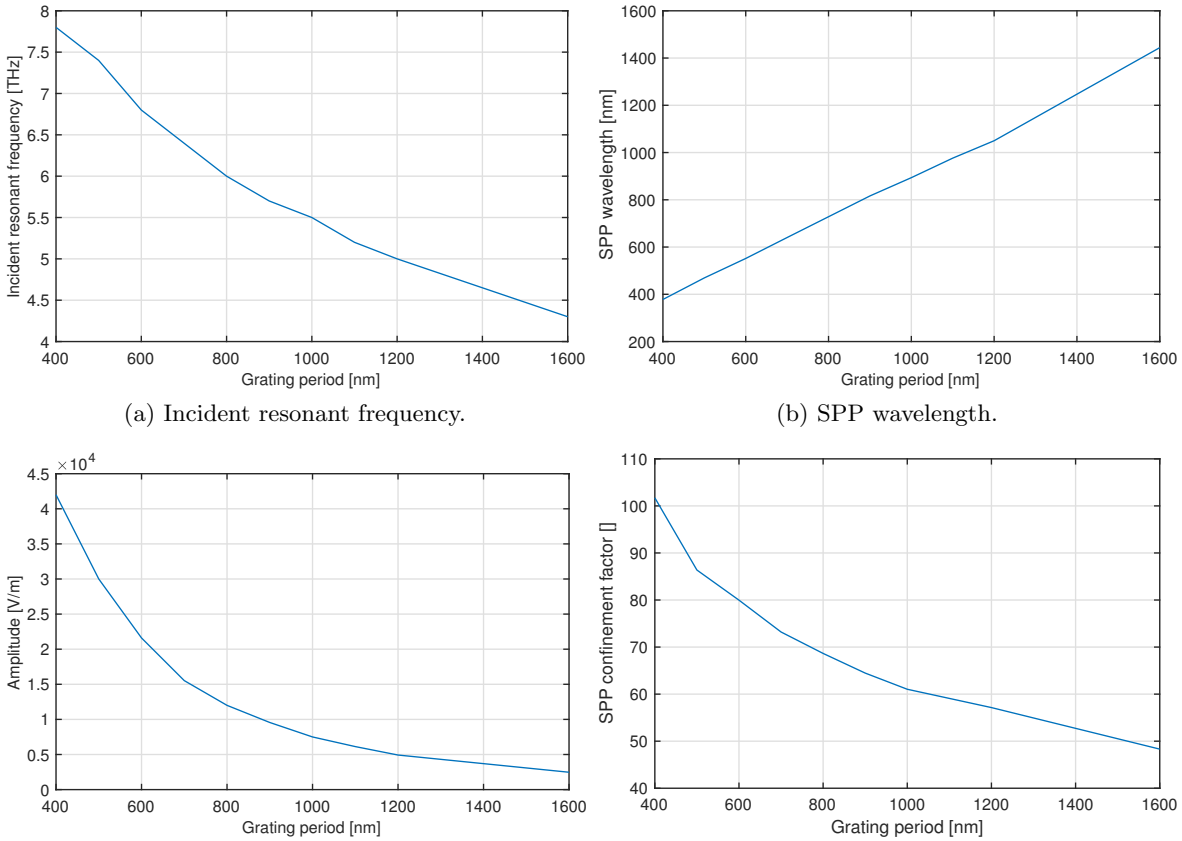

(a) Incident resonant frequency.

(b) SPP wavelength.

(c) SPP wave amplitude.

(d) SPP confinement factor.

Figure 2: Performance analysis as a function of the grating period.

thickness of 300 nm, PMMA thickness of 45 nm), but now only a fraction of the graphene layer is covered by the grating (see Figure 4a), as opposed to the previous analysis, in which a periodic boundary condition was assumed. From this analysis, we can extract the exponential decay coefficient. In Figure 4c, we plot the decay factor as a function of the Fermi energy. The decay factor decreases with the Fermi energy, as the SPP wave is less confined, similar to the previous analysis. These results show the possibility to utilize a partial grating to launch SPP waves, which can then be further processed beyond the grating.

In this section, we have shown the possibility to electrically tune the response of the grating-gated graphene-based heterostructure which can be used to launch SPP waves on graphene. In order to further understand the usefulness of such setup for THz communications, we are interested also in the modulation bandwidth or speed at which the device can be tuned. This is the objective of the next section.

3. TEMPORAL DYNAMICS OF GRAPHENE-BASED MODULATORS

In this section, we describe the process by which the Fermi energy of the graphene layer in the proposed plasmonic heterostructures (Figure 1) can be tuned, and we numerically investigate the Fermi energy achievable and modulation bandwidth.

3.1 Interfacial Charge Transfer in Graphene Heterostructures

The deposition of graphene on a metal results in a shift of the graphene Fermi-level away from charge neutrality.[36] This is the result of electrostatic doping, i.e., the process by which electrons transfer from the lower work function metal to the higher work function graphene, resulting in n-type doping of the graphene layer (i.e., graphene is doped with excess electrons). One would expect no charge doping when graphene is placed on a metal having

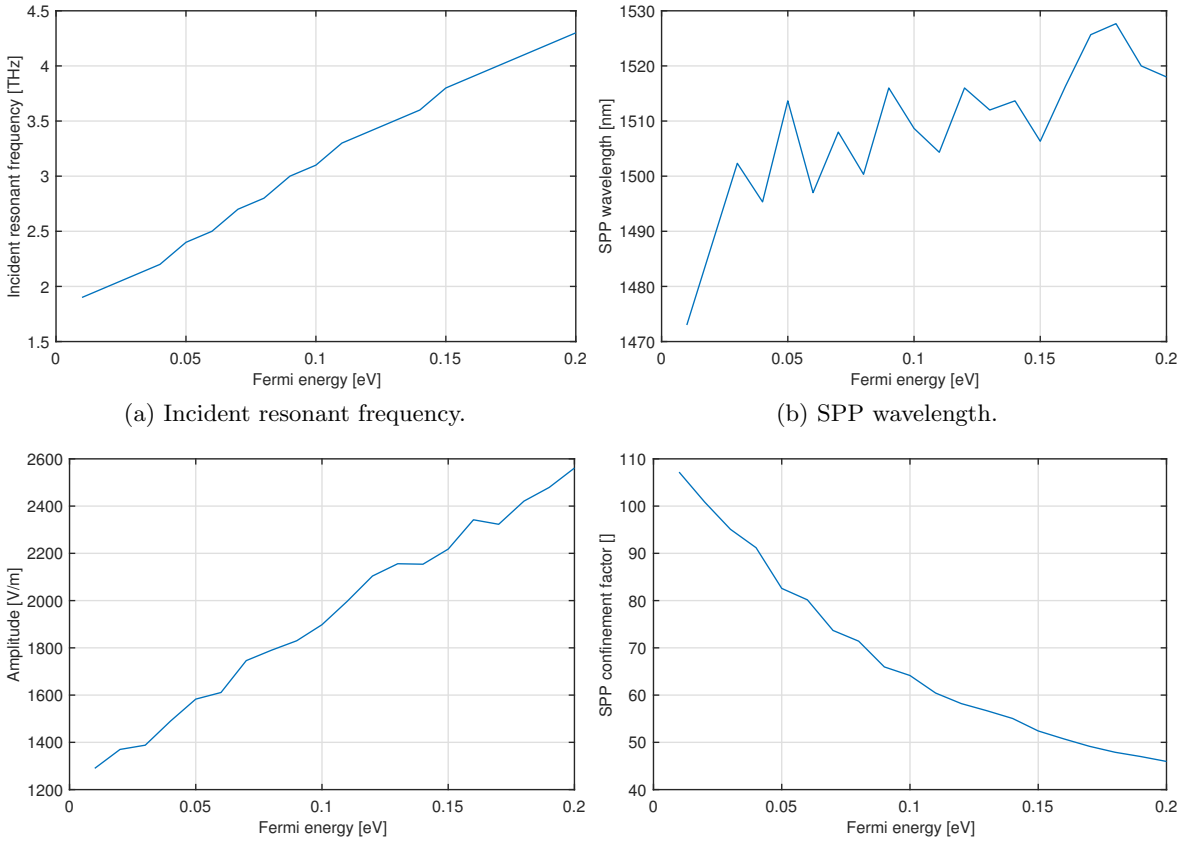

(a) Incident resonant frequency.

(b) SPP wavelength.

(c) SPP wave amplitude.

(d) SPP confinement factor.

Figure 3: Performance analysis as a function of the Fermi energy.

an equal work function, however, this has been shown to result in n-type doping. This is due to the dipolar moment that is induced at the interface between graphene and the metal, which effectively lowers the metal's work function, allowing electrons to escape the metal surface and transfer into graphene more easily. Even for weakly interacting materials, the induced dipole is an intrinsic property of interfaces and can be of significant magnitude.[37]

An analogous type of charge transfer is observed when graphene is supported on dielectric/insulating substrates, as well as when a dielectric material is sandwiched in between graphene and a metal substrate. Inserting a dielectric layer between graphene and a metal substrate reduces the amount of charge doping by creating an energy barrier, but some electrons are still able to tunnel into graphene. This ultimately depends on the thickness of the dielectric layer. While dielectric thickness of several tens of nanometers are common (e.g., 45 nm in the devices analyzed in Section 2), the use of two dimensional dielectric materials, such as boron nitride (h-BN), enables the creation of ultra-thin dielectric layers. Both graphene and h-BN are arranged in an hexagonal lattice and have very similar lattice constant, which allows graphene to rest on h-BN with as little perturbation of its electronic structure as possible.[37] We will take this into consideration in the next sections.

3.2 Electric Field Modulation of Charge Transfer

The charge doping processes in graphene/dielectric/metal structures can be controlled by applying a gate voltage to the dielectric layer. This voltage essentially increases (decreases) the energy barrier within the dielectric layer, making it harder (simpler) for electrons to be transferred from the metal to graphene.

Graphene has a very low density of electronic states, so relatively small changes in its charge doping can cause a significant change in its Fermi-level. Since the conductivity of graphene is a function of its Fermi-level,

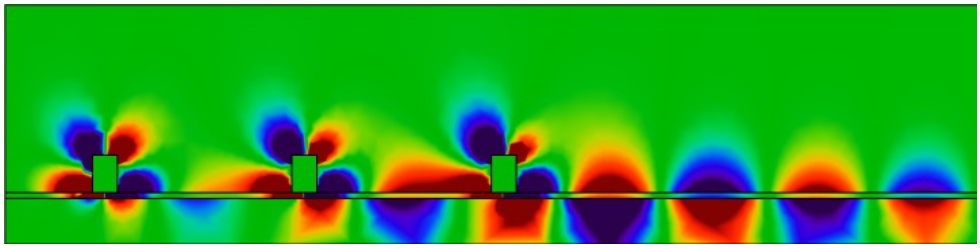

(a) Partial grating structure and resulting fields.

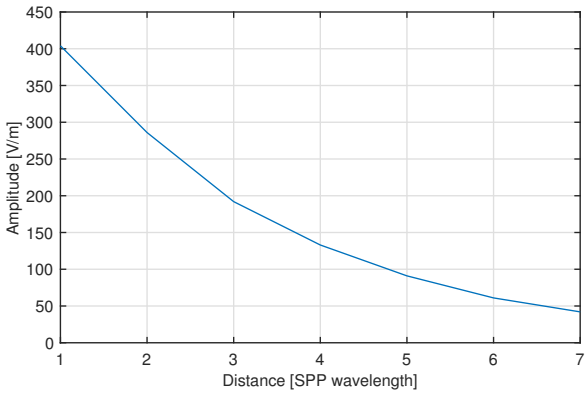

(b) Amplitude as a function of distance

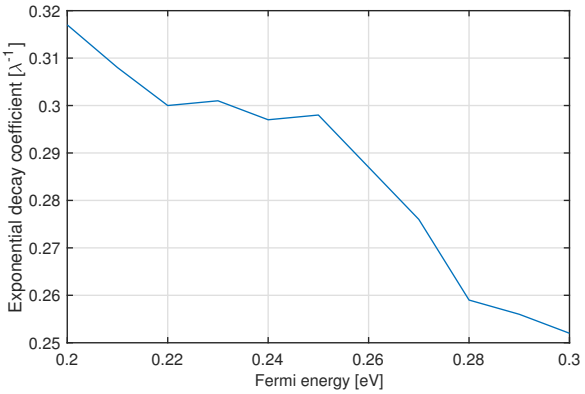

(c) Decay as a function of Fermi energy

Figure 4: Impact of Fermi energy on the SPP wave propagation length.

the application of a gate voltage can yield significant control over the conductivity. The change in Fermi-energy E_F with an applied gate voltage V_g is given by[37]

$$\triangle E_F = \pm \frac{\sqrt{1 + 2\alpha D_0 d \left|V_g - V_0\right| / \varepsilon_r} - 1}{\alpha D_0 d / \varepsilon_r}, \tag{5}$$

where d and ε_r are the thickness and relative permittivity of the dielectric layer, D_0=0.102 /eV^2 and $\alpha = e^2/(\varepsilon_0 A)$ with A=5.18 Å^2. In Figure 5, we illustrate the Fermi energy of a graphene layer on top of a metallic gate with a variable number of layers of boron nitride ($\varepsilon_r = 2.8$) in between and as a function of the gate voltage. When utilizing thinner dielectric (i.e., a fewer number of layers), for the same voltage sweep, the range of achievable Fermi energies is much higher. The larger the Fermi energy range, the larger the graphene's conductivity range and, thus, the more tunable the device is. This motivates the utilization of thinner dielectrics for larger tunability.

3.3 Time-scale for Modulating the Fermi-level

In addition to the range of achievable Fermi energies, we are interested in the time needed for the graphene layer to achieve a target value. This will set a fundamental limit on the achievable modulation bandwidth of plasmonic devices. As a first estimate, we can think of the graphene/dielectric/metal heterostructure as a parallel plate capacitor. Consequently, the time-scale for modulating the charge and, thus, the Fermi energy of the graphene layer, can be estimated using the RC time constant. Although electron transport in graphene is almost ballistic in nature, the quantum or contact resistance of graphene is not negligible, and can be quite large for graphene nanoribbons having only a few conducting bands. The contact resistance R_Q can be estimated as:[38]

$$R_Q = \frac{h}{2e^2 M}, \tag{6}$$

where h is the Planck's constant, e is the electron charge and M is the number of conducting bands, which can be estimated from the energy band-structure of graphene. This resistance decreases rapidly with increasing the nanoribbon width and Fermi-level, due to the number of conducting bands increasing with both of these two

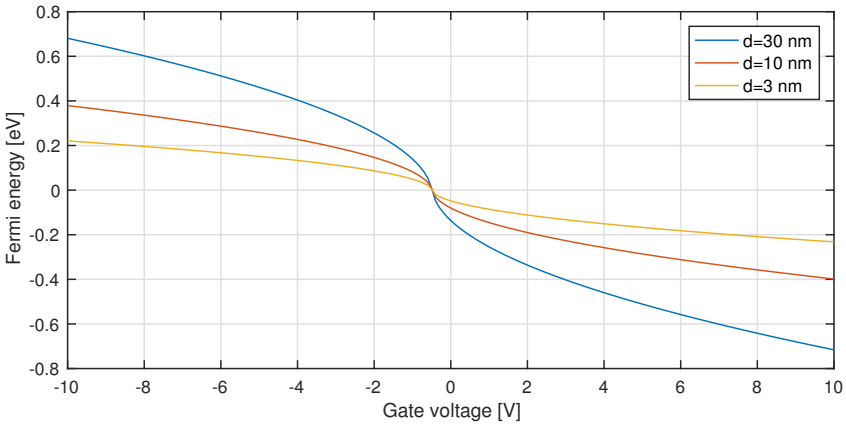

Figure 5: Change in Fermi-energy as a function of gate voltage, for various dielectric thicknesses.

magnitudes. In our devices, we consider relatively large graphene sheets (1 µm by 100 nm) which exhibit small contact resistance (approximately 100 Ω).

There are two major capacitances to consider when calculating the total capacitance C^T of a graphene sheet, namely, the quantum capacitance C_Q and electrostatic capacitance C_E:[38]

$$C^T = \left(1/C_Q^T + 1/C_E\right)^{-1}, \tag{7}$$

$$C_Q^T = \sum_{n=1}^{M} C_Q, \text{ with } C_Q = 4e^2/\left(hV_F\right) \tag{8}$$

$$C_E = \varepsilon_0 \varepsilon_r A/d, \tag{9}$$

where v_F is the Fermi-velocity, $\varepsilon_0\varepsilon_r$ is the permittivity of the dielectric, d is the thickness of the dielectric, and A is the area of the graphene sheet. The quantum capacitance can be calculated by treating the conducting bands in a graphene sheet as individual sets of capacitors in parallel, and it greatly increases as the number of conducting bands increases. The electrostatic capacitance is primarily a function of the dielectric thickness and the graphene sheet area, and is generally much smaller than the quantum capacitance. By taking into account that the quantum and electrostatic capacitances are in series, it is apparent that the much smaller electrostatic capacitance dominates the total capacitance.

In Figure 6, we illustrate the charging curve for or a 1 µm by 100 nm graphene layer on boron nitride and copper, for different dielectric thicknesses and as a function of the target voltage. While always in the sub-picosecond level, thicker dielectric layers result in lower charging times and, potentially, higher modulation bandwidth in the proposed plasmonic devices. Therefore, in light of the observations in Sections 3.1 and 3.3, it is evident that there is a compromise between tunability and modulation bandwidth, which needs to be determined in light of the target application.

4. CONCLUSION

In this paper, we have investigated the tunability of grating-gated graphene-based plasmonic heterostructures for THz band communication. First, we have analytically and numerically modeled the impact of the graphene layer Fermi energy on the the resonant frequency, amplitude and propagation length of SPP waves excited on the graphene layer through the metallic grating. Second, we have analytically modeled process by which the Fermi energy can be modified and numerically estimated the modulation bandwidth or rate at which the Fermi energy can be changed in the proposed structures, for different dielectric thicknesses. The results further motivate the use of grating-gated graphene-based heterostructures as tunable SPP wave sources, modulators and detectors, with modulation bandwidths that can satisfy the target needs in THz communication systems.

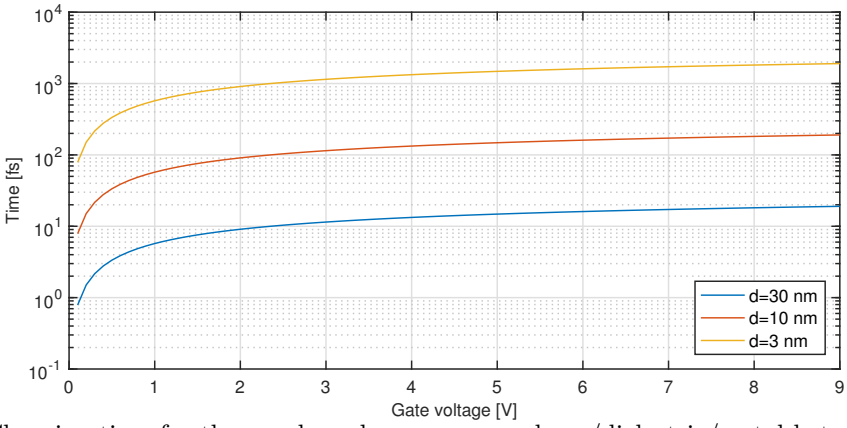

Figure 6: Charging time for the graphene layer on a graphene/dielectric/metal heterostructure.

ACKNOWLEDGMENTS

This work was completed with the support of the AFRL Information Directorate Summer Internship program. This work was also partially supported by the Air Force Office of Scientific Research (AFOSR) under Grant FA9550-16-1-0188.

REFERENCES

[1] Cherry, S., "Edholm's law of bandwidth," *IEEE Spectrum* **41**, 58–60 (July 2004).

[2] Rappaport, T., Murdock, J., and Gutierrez, F., "State of the art in 60-GHz integrated circuits and systems for wireless communications," *Proceedings of the IEEE* **99**, 1390–1436 (Aug. 2011).

[3] Khalighi, M. A. and Uysal, M., "Survey on free space optical communication: A communication theory perspective," *IEEE Communications Surveys Tutorials* **16**, 2231–2258 (Fourthquarter 2014).

[4] Federici, J. and Moeller, L., "Review of terahertz and subterahertz wireless communications," *Journal of Applied Physics* **107**(11), 111101 (2010).

[5] Song, H.-J. and Nagatsuma, T., "Present and future of terahertz communications," *IEEE Transactions on Terahertz Science and Technology* **1**(1), 256–263 (2011).

[6] Akyildiz, I. F., Jornet, J. M., and Han, C., "Terahertz band: Next frontier for wireless communications," *Physical Communication (Elsevier) Journal* **12**, 16–32 (Sept. 2014).

[7] Kurner, T. and Priebe, S., "Towards THz Communications-Status in Research, Standardization and Regulation," *Journal of Infrared, Millimeter, and Terahertz Waves* **35**(1), 53–62 (2014).

[8] Jornet, J. M. and Akyildiz, I. F., "Channel modeling and capacity analysis of electromagnetic wireless nanonetworks in the terahertz band," *IEEE Transactions on Wireless Communications* **10**, 3211–3221 (Oct. 2011).

[9] Koenig, S., Lopez-Diaz, D., Antes, J., Boes, F., Henneberger, R., Leuther, A., Tessmann, A., Schmogrow, R., Hillerkuss, D., Palmer, R., et al., "Wireless sub-THz communication system with high data rate," *Nature Photonics* **7**(12), 977–981 (2013).

[10] Kurita, Y., Ducournau, G., Coquillat, D., Satou, A., Kobayashi, K., Tombet, S. B., Meziani, Y., Popov, V., Knap, W., Suemitsu, T., et al., "Ultrahigh sensitive sub-terahertz detection by InP-based asymmetric dual-grating-gate high-electron-mobility transistors and their broadband characteristics," *Applied Physics Letters* **104**(25), 251114 (2014).

[11] Radisic, V., Leong, K., Scott, D., Monier, C., Mei, X., Deal, W., and Gutierrez-Aitken, A., "Sub-millimeter wave InP technologies and integration techniques," in [*IEEE MTT-S International Microwave Symposium (IMS)*], 1–4 (May 2015).

[12] Williams, B. S., "Terahertz quantum-cascade lasers," *Nature photonics* **1**(9), 517–525 (2007).

[13] Lu, Q., Slivken, S., Bandyopadhyay, N., Bai, Y., and Razeghi, M., "Widely tunable room temperature semiconductor terahertz source," *Applied Physics Letters* **105**(20), 201102 (2014).

[14] Lu, Q., Wu, D., Sengupta, S., Slivken, S., and Razeghi, M., "Room temperature continuous wave, monolithic tunable THz sources based on highly efficient mid-infrared quantum cascade lasers," *Scientific reports* **6** (2016).

[15] Dyakonov, M. and Shur, M. S., "Current instability and plasma waves generation in ungated two-dimensional electron layers," *Applied Physics Letters* **87**(11), 111501 (2005).

[16] Knap, W., Teppe, F., Dyakonova, N., Coquillat, D., and Lusakowski, J., "Plasma wave oscillations in nanometer field effect transistors for terahertz detection and emission," *Journal of Physics: Condensed Matter* **20**(38), 384205 (2008).

[17] Otsuji, T., Watanabe, T., Boubanga Tombet, S., Satou, A., Knap, W., Popov, V., Ryzhii, M., and Ryzhii, V., "Emission and detection of terahertz radiation using two-dimensional electrons in III-V semiconductors and graphene," *IEEE Transactions on Terahertz Science and Technology* **3**(1), 63–71 (2013).

[18] Geim, A. K. and Novoselov, K. S., "The rise of graphene," *Nature Materials* **6**, 183–191 (Mar. 2007).

[19] Novoselov, K. S., Fal, V., Colombo, L., Gellert, P., Schwab, M., Kim, K., et al., "A roadmap for graphene," *Nature* **490**(7419), 192–200 (2012).

[20] Ferrari, A. C., Bonaccorso, F., Fal'Ko, V., Novoselov, K. S., Roche, S., Bøggild, P., Borini, S., Koppens, F. H., Palermo, V., Pugno, N., et al., "Science and technology roadmap for graphene, related two-dimensional crystals, and hybrid systems," *Nanoscale* **7**(11), 4598–4810 (2015).

[21] Ju, L., Geng, B., Horng, J., Girit, C., martin, M., Hao, Z., Bechtel, H., Liang, X., Zettl, A., Shen, Y. R., and Wang, F., "Graphene plasmonics for tunable terahertz metamaterials," *Nature Nanotechnology* **6**, 630–634 (Sept. 2011).

[22] Jornet, J. M. and Akyildiz, I. F., "Graphene-based plasmonic nano-transceiver for terahertz band communication," in [*Proc. of European Conference on Antennas and Propagation (EuCAP)*], (2014).

[23] Dyakonov, M. and Shur, M., "Shallow water analogy for a ballistic field effect transistor: New mechanism of plasma wave generation by dc current," *Phys. Rev. Lett.* **71**, 2465–2468 (Oct. 1993).

[24] Cleary, J. W., Peale, R. E., Saxena, H., and Buchwald, W. R., "Investigation of plasmonic resonances in the two-dimensional electron gas of an ingaas/inp high electron mobility transistor," in [*SPIE Defense, Security, and Sensing*], 80230X–80230X, International Society for Optics and Photonics (2011).

[25] Esfahani, N. N., Cleary, J. W., Peale, R. E., Buchwald, W. R., Fredricksen, C. J., Hendrickson, J., Lodge, M. S., Dawson, B. D., and Ishigami, M., "Inp-and graphene-based grating-gated transistors for tunable thz and mm-wave detection," in [*SPIE Defense, Security, and Sensing*], 837327–837327, International Society for Optics and Photonics (2012).

[26] Sensale-Rodriguez, B., Yan, R., Kelly, M. M., Fang, T., Tahy, K., Hwang, W. S., Jena, D., Liu, L., and Xing, H. G., "Broadband graphene terahertz modulators enabled by intraband transitions," *Nature Communications* **3**, 780+ (Apr. 2012).

[27] Lee, S. H., Kim, H.-D., Choi, H. J., Kang, B., Cho, Y. R., and Min, B., "Broadband modulation of terahertz waves with non-resonant graphene meta-devices," *IEEE Transactions on Terahertz Science and Technology* **3**(6), 764–771 (2013).

[28] Singh, P. K., Aizin, G., Thawdar, N., Medley, M., and Jornet, J. M., "Graphene-based plasmonic phase modulator for terahertz-band communication," in [*Proc. of the European Conference on Antennas and Propagation (EuCAP)*], *to appear in Proc. of European Conference on Antennas and Propagation* (2016).

[29] Falkovsky, L. and Varlamov, A. A., "Space-time dispersion of graphene conductivity," *The European Physical Journal B* **56**, 281–284 (2007).

[30] Hanson, G. W., "Dyadic Green's functions and guided surface waves for a surface conductivity model of graphene," *Journal of Applied Physics* **103**(6), 064302 (2008).

[31] Allen Jr, S., Tsui, D., and Logan, R., "Observation of the two-dimensional plasmon in silicon inversion layers," *Physical Review Letters* **38**(17), 980 (1977).

[32] Peres, N., Bludov, Y. V., Ferreira, A., and Vasilevskiy, M. I., "Exact solution for square-wave grating covered with graphene: surface plasmon-polaritons in the terahertz range," *Journal of Physics: Condensed Matter* **25**(12), 125303 (2013).

[33] COMSOL Multiphysics Simulation Software, "COMSOL."

[34] Johnson, P. B. and Christy, R.-W., "Optical constants of the noble metals," *Physical Review B* **6**(12), 4370 (1972).

[35] Jornet, J. M. and Akyildiz, I. F., "Graphene-based plasmonic nano-antenna for terahertz band communication in nanonetworks," *IEEE JSAC, Special Issue on Emerging Technologies for Communications* **12**, 685–694 (Dec. 2013).

[36] Dahal, A. and Batzill, M., "Graphene–nickel interfaces: a review," *Nanoscale* **6**(5), 2548–2562 (2014).

[37] Bokdam, M., Khomyakov, P. A., Brocks, G., and Kelly, P. J., "Field effect doping of graphene in metal—dielectric— graphene heterostructures: A model based upon first-principles calculations," *Physical Review B* **87**(7), 075414 (2013).

[38] Jornet, J. M. and Akyildiz, I. F., "Graphene-based nano-antennas for electromagnetic nanocommunications in the terahertz band," in [*Proc. of 4th European Conference on Antennas and Propagation, EUCAP*], (Apr. 2010).